

Hydrothermal synthesis of NiS nanobelts and NiS₂ microspheres constructed of cuboids architectures

Lili Wang, Yongchun Zhu*, Haibo Li, Qianwen Li, Yitai Qian*

Department of Chemistry, Hefei National Laboratory for Physical Sciences at Microscale, University of Science and Technology of China, Hefei, Anhui 230026, China

ARTICLE INFO

Article history:

Received 28 July 2009

Received in revised form

20 October 2009

Accepted 25 October 2009

Available online 31 October 2009

Keywords:

Nickel sulfide

Nanobelts

Microspheres

Hydrothermal

Crystal growth

ABSTRACT

NiS nanobelts of hexagonal phase have been hydrothermally synthesized starting from Ni(CH₃COO)₂·4H₂O and Na₂S₂O₃·5H₂O at 200 °C for 12 h. The as-prepared nanobelts were 50 nm thick, 70–200 nm wide and more than 10 μm long. As ethylenediaminetetraacetic acid (EDTA) added, in similar condition, 2 μm NiS₂ microspheres of cubic phase were prepared. However, as Ni²⁺/S₂O₃²⁻ ratio was 1:1 and the temperature was decreased to 160 °C, 5 μm NiS₂ microspheres constructed of cuboids were formed.

© 2009 Elsevier Inc. All rights reserved.

1. Introduction

Nickel sulfides can form various phases such as NiS, Ni_{3+x}S₂, Ni₃S₂, Ni₇S₆, Ni₉S₈, Ni₃S₄, and NiS₂. NiS exhibits two phases: the hexagonal phase [1] and rhombohedral phase [2]. Both hexagonal and rhombohedral NiS have attractive electrical [3,4] and catalytic activity [5] properties and can be used in various fields such as IR detectors [6], cathode materials in rechargeable lithium batteries [7] and hydrodesulfurization catalyst [8,9]. Hexagonal NiS also presents metal-semiconductor [10], paramagnetic-antiferromagnetic transition properties [11]. Various morphologies of rhombohedral NiS has been synthesized, such as chain-like tubes [12], layer-rolled [13], urchin-like [14] and flower-like [15] structures. Rhombohedral NiS nanorods and triangular nanoprisms have been synthesized by solventless thermolytic decomposition of nickel thiolate precursors [2]. The length of NiS nanorods was ranging from 15 to 50 nm and typically with aspect ratios of approximately 4. Hexagonal NiS of irregular crystalline particles [16] and nanocrystalline [17] were prepared in water and ethanol by our group in 2001. Later, sea-urchin-like of hexagonal NiS [18] synthesized in hydrazine hydrate was reported.

NiS₂ holds a triclinic phase [19] and a cubic phase [20]. And it is reported that cubic NiS₂ possesses electronic [3], magnetic [21] and optical [22] characteristics. Dendritic NiS₂ nanostructures of cubic phase have been synthesized by using γ -irradiation method [22]. Through a solvothermal synthetic route, monodisperse NiS₂

dodecahedrons and microspheres with a diameter of 6 μm [23] and cubic shaped NiS₂ [24] have been synthesized.

In this study, NiS nanobelts of hexagonal phase were prepared by the direct reaction of Ni(CH₃COO)₂·4H₂O and Na₂S₂O₃·5H₂O in aqueous solution at 200 °C for 12 h with Ni²⁺/S₂O₃²⁻ molar ratio of 2:1. By introducing EDTA in the reaction, NiS₂ microsphere of cubic phase could be fabricated. However, as Ni²⁺/S₂O₃²⁻ ratio was 1:1 and the temperature decreased to 160 °C, the microspheres of cubic phase NiS₂ were constructed of cuboids.

2. Experimental Section

All reagents were of analytical grade and without further purification. In a typical synthesis procedure for NiS nanobelts, 2 mmol of Ni(CH₃COO)₂·4H₂O and 1 mmol of Na₂S₂O₃·5H₂O were ordinarily dissolved with 40 mL of distilled water in a beaker. After being stirred for 10 min, the mixture was transferred to a 50 mL Teflon-lined autoclave. Then the autoclave was sealed and heated at 200 °C for 12 h. After the reaction, the autoclave was allowed to cool to room temperature naturally. The obtained black products were collected by centrifugation and washed several times with distilled water and anhydrous ethanol. Finally the products were dried under vacuum at 60 °C. For the synthesis of cubic NiS₂ microspheres, a similar procedure was performed except for the introduction of ethylenediaminetetraacetic acid (EDTA) in reaction system.

X-ray powder diffraction (XRD) patterns of the products were obtained on a Philips X'pert X-ray diffractometer with CuK α

* Corresponding authors. Fax: +86 551 3607402.

E-mail addresses: ychzhu@ustc.edu.cn (Y. Zhu), yqtian@ustc.edu.cn (Y. Qian).

radiation ($\lambda=1.54178\text{ \AA}$). The scanning electron microscopy (SEM) images were taken by using a field-emitting scanning electron microscope (FESEM, JEOL-JSM-6700F). The transmission electron

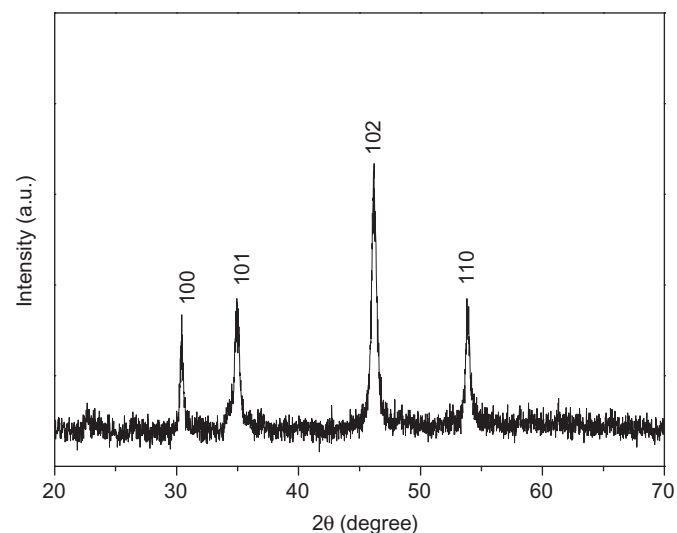


Fig. 1. XRD pattern of NiS prepared at 200 °C for 12 h without EDTA ($\text{Ni}^{2+}/\text{S}_2\text{O}_3^{2-}$ ratio was 2:1).

microscopy (TEM) images, high-resolution transmission electron microscopy (HRTEM) images and an energy-dispersive X-ray (EDX) spectrum were taken on a JEOL-2010 transmission electron microscope with an accelerating voltage of 200 kV. The photoluminescence (PL) spectra were performed on a Hitachi 850-luminescence spectrophotometer with a Xe lamp ($\lambda_{\text{ex}}=277\text{ nm}$) at room temperature.

3. Results and Discussion

3.1. Structure and morphology characterization of NiS

Fig. 1 shows the typical XRD pattern of the product prepared at 200 °C in the absence of EDTA ($\text{Ni}^{2+}/\text{S}_2\text{O}_3^{2-}$ molar ratio was 2:1). All peaks can be clearly indexed as hexagonal NiS with the cell constant $a=3.420\text{ \AA}$, $c=5.300\text{ \AA}$, which is consistent with the literature data (JCPDS Card no. 75-0613, space group $P6_3/mmc$).

Fig. 2a shows the overall morphology of hexagonal NiS nanobelts, which reveals the high yield of products. From the SEM image in **Fig. 2b**, it can be seen that the nanobelts are 50 nm in thickness, 70–200 nm in width and around 10 μm in length. The TEM images in **Fig. 2c** and **d** further confirm that the as-prepared products are nanobelts. **Fig. 2e** shows the HRTEM image of a single nanobelt corresponding to **Fig. 2d**. The interplanar spacing of

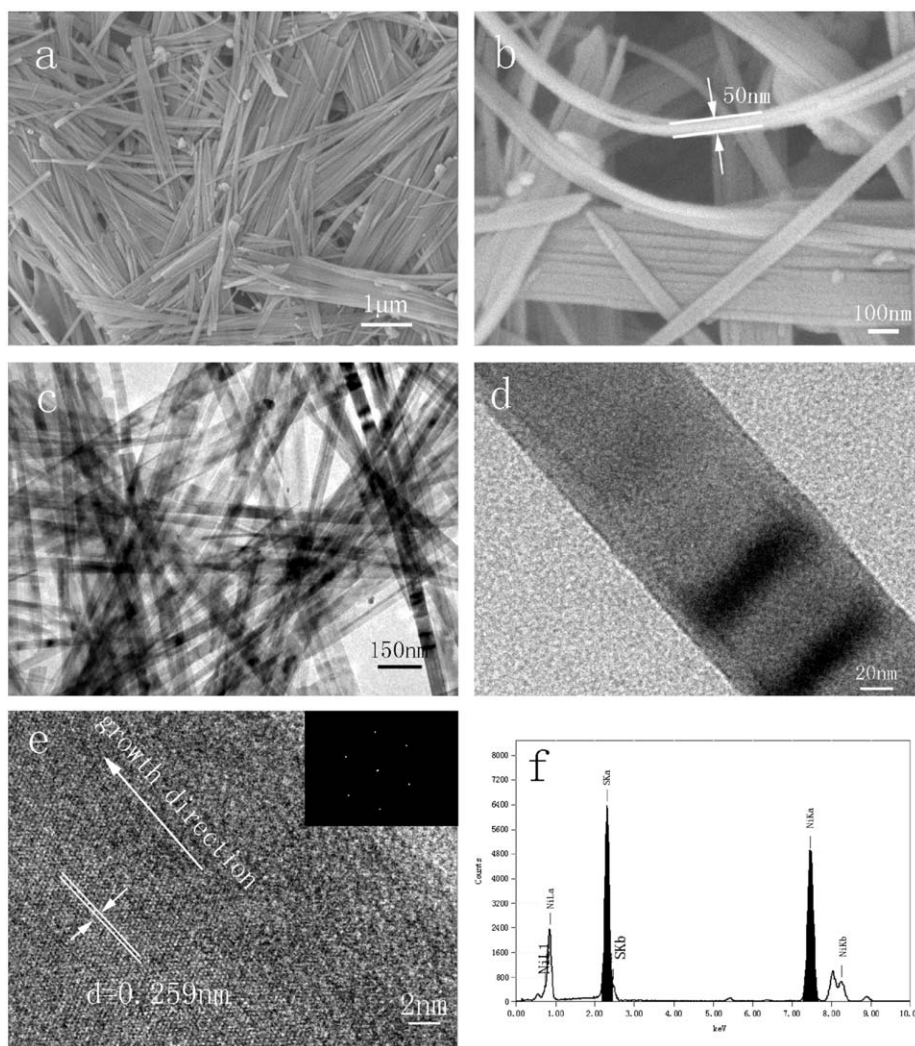


Fig. 2. Hexagonal NiS nanobelts obtained at 200 °C for 12 h without EDTA ($\text{Ni}^{2+}/\text{S}_2\text{O}_3^{2-}$ ratio was 2:1): (a) low-magnification SEM image of NiS, (b) high-magnification SEM image of NiS, (c–d) TEM images of NiS, (e) HRTEM image of the single NiS nanobelt edge in **Fig. 2d** and the corresponding FFT patterns (inset), and (f) EDX spectrum of NiS.

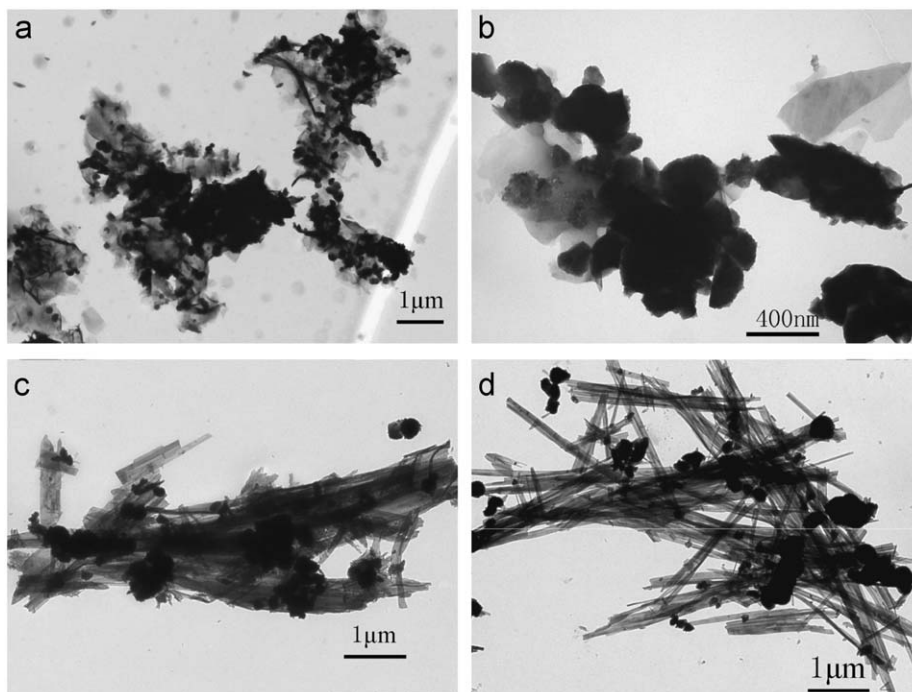


Fig. 3. TEM images of NiS collected at different stages: (a) 1 h, (b) 2 h, (c) 3 h, and (d) 6 h.

0.259 nm matches well with the distance between the (101) crystal planes of hexagonal NiS. It can be seen that the nanobelt grows along the direction parallel to the (101) crystal planes. Both the HRTEM image and fast-fourier-transform (FFT) ED (inset of Fig. 2e) indicate NiS nanobelts are single-crystalline. Besides, EDX analysis (Fig. 2f) was also applied to determine the chemical composition of the sample. Only nickel and sulfide elements are detected with a molar ratio of about 1:1.08 (Ni:S), which further confirms that the as-prepared products are NiS.

3.2. Growth mechanism of NiS nanobelts

For understanding the growth mechanism of NiS nanobelts, the intermediate products at different reaction stages (1, 2, 3 and 6 h) have been studied by TEM technique. The TEM images shown in Fig. 3 reveal the transition process from nanoparticles to nanobelts. Fig. 3a shows that only nanoparticles can be observed at a reaction time of 1 h. After reacting for 2 h, nanoparticles were still the main products accompanied by some nanoflakes (Fig. 3b). Subsequently, the aggregated nanobelts (Fig. 3c) began to take shape with reaction time up to 3 h. When the time was prolonged to 6 h, the nanobelts became the predominant products. And at a time of 12 h, almost all the products became nanobelts. The procedure investigation suggests that the NiS nanobelts grow at the expenses of small nanoparticles. The nuclei aggregation progress and the nanobelts growth progress by consuming small nanoparticles and it is a typical Ostwald ripening process [25]. In the homogeneous solution system, many NiS nucleated yielding nanoparticles well-dispersed in the solution. When this dispersion of nanoparticles was continuously heated at high temperatures, the small nanoparticles progressively disappeared to the benefit of larger ones. Herein, the nanobelts and larger nanoflakes may take shape [26]. In this work, nanobelts were the main products, because hexagonal NiS crystals were preferable for the anisotropic growth of crystals and finally nanobelts with high aspect ratios formed due to the anisotropic growth of crystals [27]. A further study of this issue is under way.

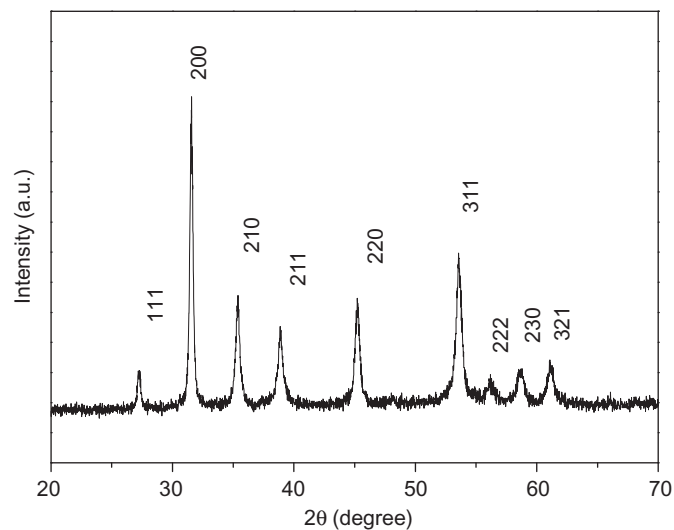


Fig. 4. XRD pattern of NiS₂ prepared at 200 °C for 12 h with EDTA (Ni²⁺/S₂O₃²⁻ ratio was 2:1).

3.3. Structure and morphology characterization of NiS₂

Keeping other experiment conditions unchanged, the reaction was undergoing in the presence of EDTA. The XRD pattern (as shown in Fig. 4) of the as-prepared products is in agreement with cubic NiS₂ (JCPDS Card no. 11-0099, space group Pa3) with the cell constant $a=5.670 \text{ \AA}$.

Fig. 5a shows the SEM image of cubic NiS₂ products prepared at 200 °C, and it can be observed that the microspheres are rugged and have an average diameter of 2 μm. When the temperature decreased to 160 °C at a Ni²⁺/S₂O₃²⁻ ratio of 2:1 (Fig. 5b), NiS₂ microspheres with a mean diameter of 2 μm constructed of irregular cuboids were found. By adjusting the Ni²⁺/S₂O₃²⁻ ratio to 1:1 at 160 °C, the diameter of NiS₂ microspheres was about 5 μm and the constructed cuboids with a mean side length of 500 nm

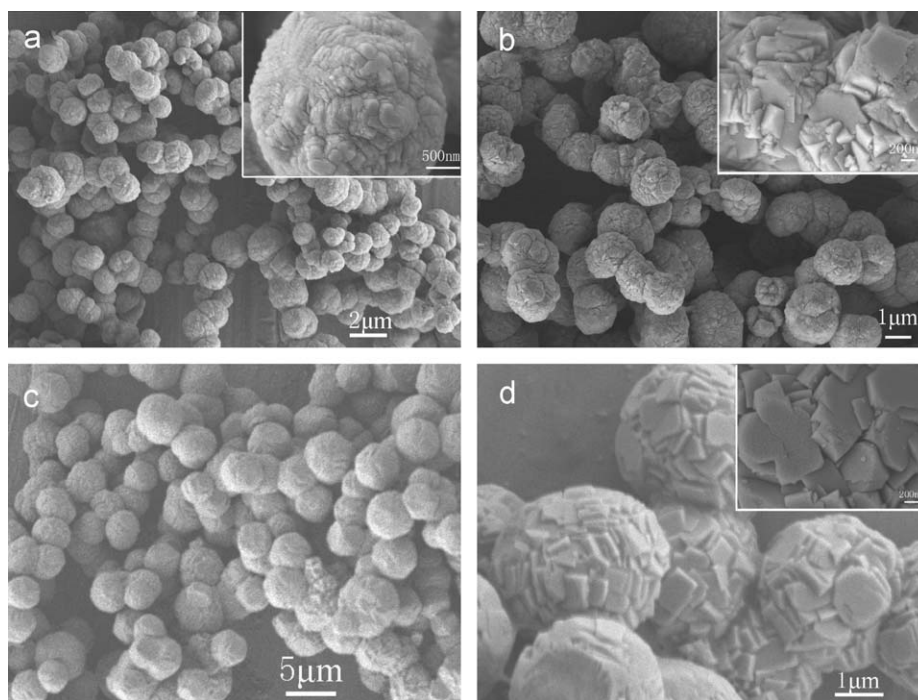


Fig. 5. SEM images of NiS₂ prepared in the presence of EDTA for 12 h, inset figure in a, b and d show high-magnification of the products. (a) 200 °C (Ni²⁺/S₂O₃²⁻ ratio 2:1), (b) 160 °C (Ni²⁺/S₂O₃²⁻ ratio 2:1), (c–d) 160 °C (Ni²⁺/S₂O₃²⁻ ratio 1:1).

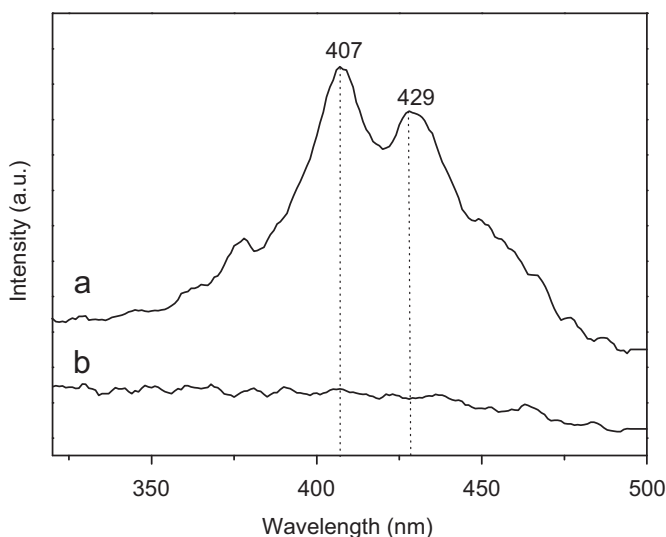


Fig. 6. Fluorescence spectrum of the products measured at room temperature at an excitation wavelength of 277 nm: (a) NiS nanobelts obtained at 200 °C for 12 h (Ni²⁺/S₂O₃²⁻ ratio was 2:1), (b) NiS₂ microspheres obtained at 160 °C for 12 h in the presence of EDTA (Ni²⁺/S₂O₃²⁻ ratio was 1:1).

became more regular. Temperature and the reactant ratio influence the crystal growth. At a higher temperature, the reactivity of the reactant is higher and the reaction speed is accelerated. The rate of NiS₂ nucleation was increased and led to a lack of time for the NiS₂ to grow up, so the nuclei aggregated and rugged microspheres formed, finally [28]. At a lower temperature, the reactivity of the reactant is low, which is beneficial to the crystal inherent growth habit. The NiS₂ obtained here was of cubic phase, then the nuclei aged and grew up to cuboids. However, insufficient S₂O₃²⁻ led to poor control on the growth rate of crystal planes and irregular cuboids were obtained. When sufficient S₂O₃²⁻ were added, the regular cuboids of NiS₂ formed [29].

4. Photoluminescent properties

The optical properties of the products were investigated. Fig. 6 shows the fluorescence spectrum of NiS nanobelts and NiS₂ microspheres under an excitation $\lambda_{\text{ex}}=277$ nm. There is a broad emission for NiS nanobelts (as shown in Fig. 6a), and the top of the emission peak is separated into two peaks located, respectively, at 407 and 429 nm, which is close to the reference reported data [15,30]. The separated peaks might be aroused by the defects in the interfacial region due to electronic transitions and may be attributed to the existence of the crystal imperfections, such as point defects, dislocations or grain boundaries in the sample of NiS nanobelts [31]. However, there is nearly no fluorescence observed for NiS₂ microspheres architectures (Fig. 6b). The characteristic differences of two fluorescence spectrum are mainly caused by the different phases, shapes their structural complexity and specialty between NiS and NiS₂ [32].

5. Conclusion

In summary, applying Ni(CH₃COO)₂ · 4H₂O and Na₂S₂O₃ · 5H₂O as the starting material, hexagonal NiS nanobelts and cubic NiS₂ microspheres have been hydrothermally synthesized. Hexagonal NiS nanobelts were prepared at 200 °C for 12 h with a Ni²⁺/S₂O₃²⁻ ratio of 2:1. When EDTA was introduced, cubic NiS₂ was obtained. By regulating the temperature to 160 °C and the Ni²⁺/S₂O₃²⁻ ratio to 1:1, cubic NiS₂ microsphere structure piled by cuboids was synthesized.

Acknowledgment

The financial support of this work, by the 973 Project of China (no. 2005CB623601), is gratefully acknowledged.

References

- [1] X.C. Sun, Appl. Surf. Sci. 217 (2003) 23–27.
- [2] A. Ghezelbash, M.B. Sigman, B.A. Korgel, Nano Lett. 4 (2004) 537–542.
- [3] J.H. Wang, Z. Cheng, J.L. Bredas, M.L. Liu, J. Chem. Phys. 127 (2007) 8.
- [4] J.L. Horwood, L.G. Ripley, M.G. Townsend, R.J. Tremblay, J. Appl. Phys. 42 (1971) 1476–1477.
- [5] V.A. Burmistrov, A.N. Startsev, Yu.I. Yermakov, React. Kinet. Catal. Lett. 22 (1982) 107–111.
- [6] F. Atay, S.K. Ose, V. Bilgin, I. Akyuz, Turk. J. Phys. 27 (2003) 285–292.
- [7] S.C. Han, K.W. Kim, H.J. Ahn, J.H. Ahn, J.Y. Lee, J. Alloys Compd. 361 (2003) 247–251.
- [8] A. Olivias, J. Cruz-Reyes, M. Avalos, V. Petranovskii, S. Fuentes, Mater. Lett. 38 (1999) 141–144.
- [9] A. Olivias, J. Cruz-Reyes, V. Petranovskii, M. Avalos, S. Fuentes, J. Vac. Sci. Technol. A 16 (1998) 3515–3520.
- [10] J.T. Sparks, T.E.D. Komoto, Rev. Mod. Phys. 40 (1968) 752.
- [11] J.T. Sparks, T. Komoto, J. Appl. Phys. 34 (1963) 1191.
- [12] Y.H. Zhang, L. Guo, L. He, K. Liu, C.P. Chen, Q. Zhang, Z.Y. Wu, Nanotechnology 18 (2007).
- [13] X.C. Jiang, Y. Xie, J. Lu, L.Y. Zhu, W. He, Y.T. Qian, Adv. Mater. 13 (2001) 1278–1281.
- [14] W.Q. Zhang, L.Q. Xu, K.B. Tang, F.Q. Li, Y.T. Qian, Eur. J. Inorg. Chem. (2005) 653–656.
- [15] H.B. Li, L.L. Chai, X.Q. Wang, X.Y. Wu, G.C. Xi, Y.K. Liu, Y.T. Qian, Cryst. Growth Des. 7 (2007) 1918–1922.
- [16] Z.Y. Meng, Y.Y. Peng, W.H. Yu, Y.T. Qian, Mater. Chem. Phys. 74 (2002) 230–233.
- [17] Z.Y. Meng, Y.Y. Peng, L.Q. Xu, Y.T. Qian, Mater. Lett. 53 (2002) 165–167.
- [18] X.H. Liu, Mater. Sci. Eng. B-Solid State Mater. Adv. Technol. 119 (2005) 19–24.
- [19] H. Deng, C. Chen, Q. Peng, Y.D. Li, Mater. Chem. Phys. 100 (2006) 224–229.
- [20] G.J. An, C.G. Liu, Y.D. Hou, X.L. Zhang, Y.Q. Liu, Mater. Lett. 62 (2008) 2643–2646.
- [21] W. Wang, S.Y. Wang, Y.L. Gao, K.Y. Wang, M. Liu, Mater. Sci. Eng. B-Solid State Mater. Adv. Technol. 133 (2006) 167–171.
- [22] R. Luo, X. Sun, L.F. Yan, W.M. Chen, Chem. Lett. 33 (2004) 830–831.
- [23] X.F. Qian, Y.D. Li, Y. Xie, Y.T. Qian, Mater. Chem. Phys. 66 (2000) 97–99.
- [24] S.L. Yang, H.B. Yao, M.R. Gao, S.H. Yu, CrystEngComm 11 (2009) 1383–1390.
- [25] Y.G. Sun, Y.D. Yin, B.T. Mayers, T. Herricks, Y.N. Xia, Chem. Mater. 14 (2002) 4736–4745.
- [26] Z.P. Liu, S. Li, Y. Yang, S. Peng, Z.K. Hu, Y.T. Qian, Adv. Mater. 15 (2003) 1946–1948.
- [27] J.T. Hu, T.W. Odom, C.M. Lieber, Acc. Chem. Res. 32 (1999) 435–445.
- [28] H.P. Cong, S.H. Yu, Cryst. Growth Des. 9 (2009) 210–217.
- [29] L.L. Wang, L. Gao, J. Phys. Chem. C 113 (2009) 15914–15920.
- [30] Z.C. Wu, C. Pan, T.W. Li, G.J. Yang, Y. Xie, Cryst. Growth Des. 7 (2007) 2454–2459.
- [31] Q.W. Chen, D.L. Zhu, C. Zhu, J. Wang, Y.G. Zhang, Appl. Phys. Lett. 82 (2003) 1018–1020.
- [32] B.X. Li, Y. Xie, Y. Xu, C.Z. Wu, Z.Q. Li, J. Solid State Chem. 179 (2006) 56–61.